An Optimized Backlight Local Dimming Algorithm for Edge-Lit LED Backlight LCDs

Seungwook Cha, Taehyeon Choi, Hoonjae Lee, and Sanghoon Sull, *Senior Member, IEEE*

***Abstract*—This paper presents an efficient optimized backlight local dimming method that minimizes power consumption under a given allowable distortion for liquid crystal displays with edge-lit light-emitting diode backlight. To reduce image quality fluctuation, an inequality constraint optimization problem is formulated using a given allowable distortion and the steepest descent method is used to solve the optimization problem. The experimental results show that the proposed method has better performance than previous methods at the same average power consumption in the unnoticeable level of the difference between the displayed images before and after dimming. Also, the proposed method reduces the risk of large performance degradation and reduces computation time by three times compared with the existing optimization based methods.**

***Index Terms*—Light-emitting diode (LED) backlight, light spread function (LSF), liquid crystal display (LCD), local dimming, optimization.**

I. Introduction

A LIQUID CRYSTAL display (LCD) with a light-emitting diode (LED) backlight is widely used in a variety of mobile devices, such as smartphones and tablet computers. Since the display consumes more battery power than other components in a mobile device [1], it is important to save its power.

Recent developments in the field of III-Nitride-based LEDs have resulted in innovations for achieving high efficiency emitters [2], [3]. These advances were driven by approaches to suppress charge separation for improved internal quantum efficiency [4]–[7], improved material epitaxy [8], [9], and suppression of the droop issue in LEDs [10]–[12]. Along with the development of new materials in LED-based backlight technology, an efficient local backlight dimming algorithm is also required to further reduce power consumption.

For an LED-backlit LCD display, there are currently two types of LED backlights, differentiated according to the position of the LEDs: direct-lit and edge-lit LED backlights [13]. The direct-lit LED backlights are placed behind a screen. On the other hand, the edge-lit LED backlights are located near the rim of the screen to reduce its thickness. A variety of backlight dimming methods for both types of LED backlights have been developed to reduce power consumption.

Existing backlight dimming algorithms can be grouped into global and local dimming approaches. First, the global dimming approaches [14]–[18] set the power of all the LEDs to the same value. They used a histogram of luminance values [14]–[17] and low-level features such as the average and maximum luminance pixel values [18]. The advantage of global dimming is that the power of LEDs can be easily controlled. Second, the local dimming methods control each LED power individually [19]–[33]. Since they analyze the image intensities around the position of each LED, they consume less power than the global dimming methods, especially for high contrast images. They usually divide an image into several blocks and then analyze low-level features such as the average and maximum luminance pixel values [19]–[27] or luminance histograms [28]–[30] to determine the power for each LED. A saliency map was also used to consider perceptual image quality [31]. However, these local dimming methods heuristically adjust the power based on neighboring blocks and the light spread from an LED light source [24]–[28] and thus do not estimate optimal power consumption. Some methods such as in [20] and [25] cannot be applied to an edge-lit LED backlight system.

Recently, an optimization problem for local dimming was formulated to minimize the weighted sum of power consumption and the distortion of an image after local dimming in the luminance component [32]. The L1-norm is used for the distortion measure to solve the optimization problem by linear programming. However, it requires greater computation since the number of variables for optimization is equal to the number of pixels in the image. An extended version of the method of [32] for the RGB color space is introduced where the optimization problem is solved using the steepest descent method with a reduced number of variables, equal to the number of LEDs. Nevertheless, for both of the methods in [32] and [33], the weight for power consumption for a given input image has to be manually adjusted in order to obtain stable image quality. For example, if a higher value of weight is used for power consumption, the distortion increases with lowered power consumption.

In this paper, we propose an efficient optimized backlight local dimming method for edge-lit LED backlight LCDs. In the proposed method, each LED's power is computed to minimize power consumption within a given allowable distortion. The proposed method uses less power than previous methods at the same average peak signal-to-noise ratio (PSNR). In the methods of [32] and [33], variations in the image quality after dimming are large with a fixed weight, and thus more power

Manuscript received November 21, 2014; revised February 04, 2015; accepted February 04, 2015. Date of publication February 09, 2015; date of current version April 07, 2015. This work was supported in part by LG Electronics, Seoul, Korea by the Basic Science Research Program through the National Research Foundation of Korea (NRF) funded by the Ministry of Education under Grant NRF-2012R1A1A2044892. *(Corresponding author: Sanghoon Sull.)*

The authors are with the School of Electrical Engineering, Korea University, Seoul 136-701, Korea (e-mail: swcha@mpeg.korea.ac.kr; thchoi@mpeg.korea.ac.kr; hoonjae@mpeg.korea.ac.kr; sull@korea.ac.kr).

Color versions of one or more of the figures are available online at http://ieeexplore.ieee.org.

Digital Object Identifier 10.1109/JDT.2015.2401604

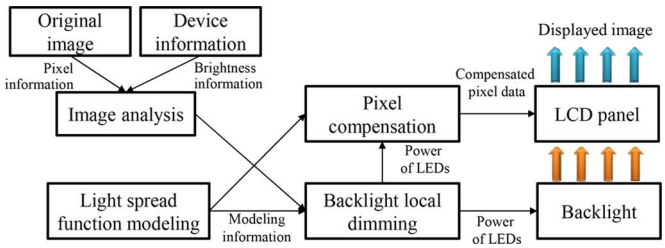

Fig. 1. Overall diagram for the proposed backlight local dimming method.

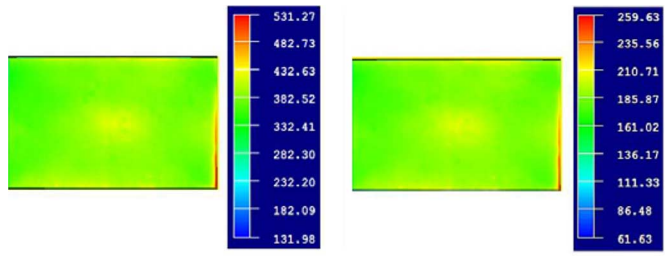

(a) (b)

Fig. 2. Backlight luminance distributions with luminance values for different power consumptions. (a) 100%. (b) 50%.

can be required for the resulting images. Since the local dimming is formulated as a constrained optimization problem in this paper, the picture quality is guaranteed to be within an allowable distortion. Moreover, the proposed method still converges faster than the latest method [33]. In our iteration process, the power of each LED is adjusted to minimize the power consumption within the given allowable distortion. The backlight luminance for each pixel is then updated by superposition of the light spread from LEDs with the adjusted power for the next iteration.

The rest of this paper is organized as follows. In Section II, we describe the proposed backlight local dimming method. In Section III, we present experimental results. Section IV concludes the paper.

II. Proposed Backlight Dimming Algorithm

We first consider an edge-lit LED backlight LCD system where K LEDs can be controlled individually. A set $\mathbf{B}$ representing the power of each LED is defined as

$$\mathbf{B} = \{B_1, B_2, \ldots, B_K\}, B_k \in [0,1], \qquad k = 1, \ldots, K \quad (1)$$

where B_k denotes the normalized power of the k-th LED. The displayed image $f_{\mathbf{c}}(\mathbf{B}, \mathbf{x})$, where $\mathbf{x}$ and $\mathbf{c}$ are the pixel position and one of the RGB components, respectively, is represented by the product of the backlight luminance $L(\mathbf{B}, \mathbf{x})$ and the liquid crystal (LC) transmittance of each color component. The value of LC transmittance is determined by converting the pixel value in the original image $I_{\mathbf{c}}(\mathbf{x})$. Therefore, we can express the displayed image as follows:

$$f_{\mathbf{c}}(\mathbf{B}, \mathbf{x}) = L(\mathbf{B}, \mathbf{x}) \cdot I_{\mathbf{c}}(\mathbf{x}) \quad (2)$$

where the value of $I_{\mathbf{c}}(\mathbf{x})$ and $L(\mathbf{B}, \mathbf{x})$ is normalized from 0 to 1. The backlight luminance $L(\mathbf{B}, \mathbf{x})$ is calculated by the summation of the product of the power B_k and the light spread function (LSF) $S_k(\mathbf{x})$, which is the influence of the k-th LED on a pixel $\mathbf{x}$:

$$L(\mathbf{B}, \mathbf{x}) = \sum_{k=1}^{K} B_k \cdot S_k(\mathbf{x}). \quad (3)$$

The process of the proposed backlight local dimming is shown in Fig. 1. First, we model the LSFs. Then, we analyze the original image with the brightness of the device and perform backlight dimming by calculating the optimal power of the LEDs using the modeled LSF. After the optimal power of the LEDs is determined, we generate the compensated image to show the displayed image to be same as before dimming. Note that we focus on making the resulting displayed image to be same as the displayed image before dimming. We now describe how to model the LSF and decide the power of the LEDs.

A. Modeling of the Light Spread Function

The LSF representing the shape of the light spread from an LED as written in (3) can take on various patterns because of the design of the light guide plate in the LCD panel [34]. The patterns can be modeled by measuring the luminance of the display using a luminance meter. We use a commercially available smartphone, which is known to use a single edge-lit LED backlight and have 10 LEDs, to measure the distribution of backlight luminance of display. Therefore, we concentrate on a single edge-lit LED backlight LCD system. Unfortunately, however, since at present mobile devices do not support controlling the power of each LED individually, we measure the distribution of backlight luminance with the same power for all LEDs using a luminance meter. For example, if the power consumption of a display is 50% of the maximum power, the power of all LEDs is equally 50%.

The distributions of backlight luminance measured under different levels of power consumption are shown in Fig. 2. We can see that the distributions of backlight luminance are almost flat and that the luminance value decreases linearly as shown in the ranges, corresponding to the reductions in power consumption. The slightly bright values in the center area (comprising 15% of the entire area) are caused by a reflection from the lens of the luminance meter. The effect of this measure error will be discussed in Section III-A. However, we do not know the exact spreading pattern from a single LED because we cannot control the power of each LED individually, as mentioned above, and the resolution of the smartphone (1280×768) is different from that of the luminance meter (490×490). Therefore, we develop three types of LSFs to model the light spreading patterns from an LED and fit them to the measured distribution of backlight luminance to determine and use a model suitable to the simulation of the proposed local dimming algorithm.

Examples of backlight distributions by the three LSFs modeled from three different patterns are shown in Fig. 3. We assume that there are three LEDs in the LCD panel on the left side and that they each have different power in order to demonstrate the differences in each pattern clearly. The first pattern is one where if an LED turns on, overall distribution of backlight luminance is almost the same (LSF 1). The LSF for this pattern is modeled as the normalized power consumption for all

(a) (b) (c)

Fig. 3. Examples of backlight distributions by three LSFs modeled from three patterns with three LEDs. (a) LSF 1. (b) LSF 2. (c) LSF 3 (proposed).

pixels. We can expect that this pattern works like global dimming. The second pattern is one where if an LED turns on, the light is spread fanwise (LSF 2). We model this pattern to the LSF using a decaying Butterworth function [35]. The last pattern is one where if an LED turns on, the light is spread in a straight forward direction without attenuation (LSF 3). We propose a new model of an LSF for this pattern by utilizing a sigmoid function to prevent the discontinuity of the distribution of backlight luminance by the differences in power between neighboring LEDs. The proposed LSF, called LSF 3, can be expressed as

$$S_k(\mathbf{x}) = \frac{1}{1+e^{-m\cdot(s(\mathbf{x})-s(\mathbf{x}_k)+n)}} + \frac{1}{1+e^{m\cdot(s(\mathbf{x})-s(\mathbf{x}_k)-n)}} - 1 \tag{4}$$

where m controls the slope of the sigmoid function and n denotes the width of the light spread. The function $s(\cdot)$ represents the position at the main axis and $\mathbf{x}_k$ is the position of the k-th LED. The main axis is defined as the axis where the LED exists. In Fig. 3(c), for instance, the main axis is the vertical axis because the LED is on the vertical line, and thus the values of the vertical axis are different by m and n, but the values of the horizontal axis are the same.

We fit these three LSFs to the measured distribution of backlight luminance to determine which LSF is suitable for the single edge-lit LED backlight.

B. Proposed Backlight Dimming Algorithm

In the proposed backlight local dimming method, an allowable distortion α is defined as the difference between the displayed images before and after dimming. If the value α is getting smaller, the displayed image after dimming will be closer to that from before dimming, but more power will be needed. Our approach is to minimize the power consumption of K LEDs under the constraint that the root mean square error of the distortion caused after backlight dimming is less than or equal to the allowable distortion α. The inequality constraint in the proposed model denotes that the relative error in each pixel is less than the allowable distortion α we set. Our approach can be written as

$$\mathbf{B}^* = \min_{\mathbf{B}} \sum_{k=1}^{K} B_k, \text{ subject to } \sqrt{\sum_{\mathbf{x}\in\mathbf{X}_s}\sum_{\mathbf{c}} \frac{1}{N_s}\cdot\left(1-\frac{f'_{\mathbf{c}}(\mathbf{B},\mathbf{x})}{f^{\text{ref}}_{\mathbf{c}}(B_{\text{flat}},\mathbf{x})}\right)^2} \le \alpha \tag{5}$$

where $\mathbf{X}_s$ is the set of positions for sampled pixels and N_s is the number of sampled pixels. The set $\mathbf{c}$ represents one of the RGB components as explained in (2). It should be noted that all pixels in the image can be used for the constraint, but to reduce the computations, the pixels in an image are uniformly sampled in the current implementation. A reference image $f^{\text{ref}}_{\mathbf{c}}(B_{\text{flat}},\mathbf{x})$ is defined as the product of the original image $I_{\mathbf{c}}(\mathbf{x})$ and the brightness of a device with a value of $B_{\text{flat}}(B_{\text{flat}}\in[0,1])$, given by a user, representing the brightness of uniform backlight luminance for all pixels. The resulting displayed image $f'_{\mathbf{c}}(\mathbf{B},\mathbf{x})$ after dimming with $\mathbf{B}$ is given by the product of the compensated image$I'_{\mathbf{c}}(\mathbf{x})$ and the backlight luminance $L(\mathbf{B},\mathbf{x})$. Thus we obtain

$$f^{\text{ref}}_{\mathbf{c}}(B_{\text{flat}},\mathbf{x}) = I_{\mathbf{c}}(\mathbf{x})\cdot B_{\text{flat}}, \tag{6}$$

$$f'_{\mathbf{c}}(\mathbf{B},\mathbf{x}) = I'_{\mathbf{c}}(\mathbf{x})\cdot L(\mathbf{B},\mathbf{x}). \tag{7}$$

The compensated image $I'_{\mathbf{c}}(\mathbf{x})$ is calculated pixel by pixel from the reference image using the backlight luminance because the LSF can exhibit a non-uniform pattern and the power of each LED is different. Also, the pixel values in the compensated image cannot be over the maximum normalized value because they are also converted to the LC transmittance, like the original image in (2). The case in which the compensated value in a pixel is over the maximum normalized value is when the pixel value of the reference image is higher than that of the backlight luminance by $\mathbf{B}$, and the distortion occurs at this pixel. This can be written as follows:

$$I'_{\mathbf{c}}(\mathbf{x}) = \begin{cases} 1, & \text{if } L(\mathbf{B},\mathbf{x}) < f^{\text{ref}}_{\mathbf{c}}(B_{\text{flat}},\mathbf{x}) \\ f^{\text{ref}}_{\mathbf{c}}(B_{\text{flat}},\mathbf{x})\cdot\frac{1}{L(\mathbf{B},\mathbf{x})}, & \text{otherwise.} \end{cases} \tag{8}$$

In (8), since the pixel values in a reference image are fixed, the backlight luminance $L(\mathbf{B},\mathbf{x})$ is affected by the power $\mathbf{B}$, and this leads to the changing of both $I'_{\mathbf{c}}(\mathbf{x})$ and $f'_{\mathbf{c}}(\mathbf{B},\mathbf{x})$. An example of the relationship between the compensated value and the resulting displayed value at a pixel $\mathbf{x}$ corresponding to the backlight luminance is shown in Fig. 4.

We can see that if the backlight luminance value $L(\mathbf{B},\mathbf{x})$ at a pixel $\mathbf{x}$ is lower than the reference value $f^{\text{ref}}_{\mathbf{c}}(B_{\text{flat}},\mathbf{x})$, the compensated value is saturated and the resulting displayed value is the same as the backlight luminance value. Therefore, the distortion occurs at this pixel. However, when a backlight luminance value is brighter than a reference value, the compensated value cannot be over the maximum normalized value, and the resulting displayed value is the same as the reference value. If there is no distortion after dimming, for instance, the resulting displayed image $f'_{\mathbf{c}}(\mathbf{B},\mathbf{x})$ should be same as the reference image.

As the proposed model is an inequality constraint problem, we can formulate this optimization problem (5) using the Lagrangian, and there exist the optimal values for $\mathbf{B}^*$ and μ^* from the Kuhn-Tucker condition [36], which is composed of the gradient equations and the complementary conditions to yield (9), shown at the bottom of the next page. Note that we removed the normalization factor and square root in the inequality constraint for computational convenience and that we can obtain K

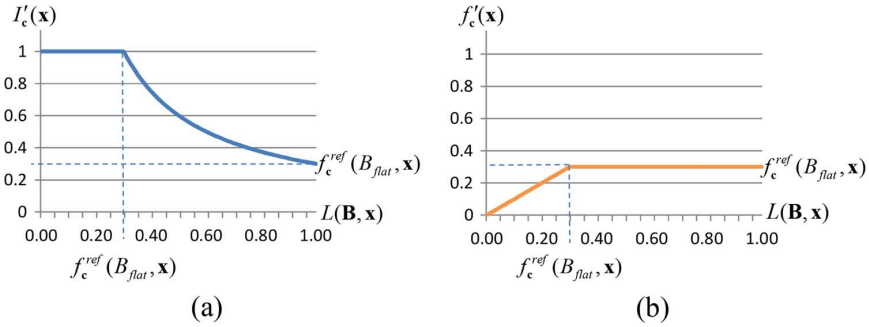

Fig. 4. Examples of the values corresponding to the backlight luminance at a pixel $\mathbf{x}$ with a reference value of 0.3. (a) Compensated value. (b) Resulting displayed value.

$+1$ nonlinear equations $g_i(\mathbf{B},\mu)$ from (9). The first K equations are from the gradient equations in the first line of (9), as given by (10), shown at the bottom of the page, where

$$\frac{\partial}{\partial B_i}\left(I'_{\mathbf{c}}(\mathbf{x})\cdot L(\mathbf{B},\mathbf{x})\right) = \begin{cases} S_i(\mathbf{x}), & \text{if } L(\mathbf{B},\mathbf{x}) < f_{\mathbf{c}}^{\text{ref}}(B_{\text{flat}},\mathbf{x}) \\ 0, & \text{otherwise} \end{cases} \tag{11}$$

and $S_i(\mathbf{x})$ represents the LSF for the i-th LED, as shown in (3). The reason that the derivative value in (11) is split is that the resulting displayed value in (7) is affected by the compensated value calculated in (8). If the derivative value is determined to be 0, there is no distortion in a color component $\mathbf{c}$ at a pixel $\mathbf{x}$. The $K+1$th equation of $g_i(\mathbf{B},\mu)$ is from the complementary condition in the second line of (9) and given by (12), shown at the bottom of the page.

To solve these nonlinear equations, we can use the following minimization problem:

$$\mathbf{B}^*,\mu^* = \min_{\mathbf{B},\mu} h(\mathbf{B},\mu) = \min_{\mathbf{B},\mu} \sum_{i=1}^{K+1} \left[g_i(\mathbf{B},\mu)\right]^2. \tag{13}$$

Then, we solve this using the steepest descent method [37] since it works well in our experiments and is computationally more efficient than Newton's method. Thus, $\mathbf{B}$ and μ are iteratively updated as

$$\mathbf{B}^{[t+1]} = \mathbf{B}^{[t]} - \delta^{[t]}\cdot \frac{\partial h}{\partial \mathbf{B}}\left(\mathbf{B}^{[t]},\mu^{[t]}\right)/z^{[t]} \tag{14}$$

$$\mu^{[t+1]} = \mu^{[t]} - \delta^{[t]}\cdot \frac{\partial h}{\partial \mu}\left(\mathbf{B}^{[t]},\mu^{[t]}\right)/z^{[t]} \tag{15}$$

where t is the number of iterations and δ is the step size descending to the minimum value. The value δ becomes small during the iteration process. The value $z^{[t]}$ is used to change the gradient of h to a unit vector:

$$z^{[t]} = \sqrt{\sum_{i=1}^{K}\left(\frac{\partial h}{\partial B_i}\left(\mathbf{B}^{[t]},\mu^{[t]}\right)\right)^2 + \left(\frac{\partial h}{\partial \mu}\left(\mathbf{B}^{[t]},\mu^{[t]}\right)\right)^2}. \tag{16}$$

The iteration stops when the changes in values are smaller than a given number and the resulting $\mathbf{B}^*$ representing the power of each LED becomes the optimal solution for (13). For all the pixels in the image, the optimized power $\mathbf{B}^*$ is applied to calculate the backlight luminance using (3), and then the compensated image is also calculated using (8).

To solve (13) using the steepest descent method, the initial power of LEDs is determined by dividing the reference image

$$\begin{aligned} \frac{\partial}{\partial \mathbf{B}}\left(\sum_{k=1}^{K} B_k + \mu\cdot\sum_{\mathbf{x}\in\mathbf{X}_s}\sum_{\mathbf{c}}\left(f_{\mathbf{c}}^{\text{ref}}(B_{\text{flat}},\mathbf{x}) - f'_{\mathbf{c}}(\mathbf{B},\mathbf{x})\right)^2\right) &= 0 \\ \mu\cdot\sum_{\mathbf{x}\in\mathbf{X}_s}\sum_{\mathbf{c}}\left(f_{\mathbf{c}}^{\text{ref}}(B_{\text{flat}},\mathbf{x}) - f'_{\mathbf{c}}(\mathbf{B},\mathbf{x})\right)^2 - \left(\alpha\cdot f_{\mathbf{c}}^{\text{ref}}(B_{\text{flat}},\mathbf{x})\right)^2 &= 0 \qquad \mu\geq 0 \end{aligned} \tag{9}$$

$$g_i(\mathbf{B},\mu) = 1 - 2\cdot\mu\cdot\left(\sum_{\mathbf{x}\in\mathbf{X}_s}\sum_{\mathbf{c}}\left(I_{\mathbf{c}}(\mathbf{x})\cdot B_{\text{flat}} - I'_{\mathbf{c}}(\mathbf{x})\cdot L(\mathbf{B},\mathbf{x})\right)\cdot\frac{\partial}{\partial B_i}\left(I'_{\mathbf{c}}(\mathbf{x})\cdot L(\mathbf{B},\mathbf{x})\right)\right) = 0, \qquad i = 1,\ldots,K \tag{10}$$

$$g_{K+1}(\mathbf{B},\mu) = \mu\cdot\sum_{\mathbf{x}\in\mathbf{X}_s}\sum_{\mathbf{c}}\left(\left(I_{\mathbf{c}}(\mathbf{x})\cdot B_{flat} - I'_{\mathbf{c}}(\mathbf{x})\cdot L(\mathbf{B},\mathbf{x})\right)^2 - \left(\alpha\cdot I_{\mathbf{c}}(\mathbf{x})\cdot B_{flat}\right)^2\right) = 0 \tag{12}$$

into K blocks and computing the histograms of the whole image and each block

$$B_k^{[0]} = \frac{P_G \cdot H_G(P_G) + \sum_{i=1}^{K} P_i \cdot H_i(P_i)}{\left(H_G(P_G) + \sum_{i=1}^{K} H_i(P_i)\right) \cdot 255} \cdot 0.5, \quad k = 1, \ldots, K, \tag{17}$$

where $B_k^{[0]}$ is the initial power of the k-th LED, K is the number of LEDs, H_G and H_i are global and local luminance histograms, respectively, and P_G and P_i are the pixel values that have the most probable luminance values in the entire image and local block, respectively. Therefore, $H_G(P_G)$ and $H_i(P_i)$ represent the probability at the most probable pixel value P_G and P_i, respectively. Also, the initial power of LEDs is determined to be the same value by using the weighted sum of luminance among each local block around an LED and the entire image.

III. Experimental Results

To more easily evaluate and compare the proposed algorithm with previous methods, we developed a simulation tool using Visual Studio 2008 and Matlab on the PC environment of Microsoft Windows 7 with Intel Core i7, 2.93 Ghz. In the simulation tool, we can set some configurations such as the displaying resolution, the number of LEDs, and the shape of modeled LSFs. We also collected 200 images as the test image set for the performance evaluation, where more than half of the 200 test images were from widely used standard test images [38]–[41] and others were the images we captured from the display screens of smartphones. The image resolution was 1280×768, and the number of LEDs was set to 10. Also, the user-defined brightness of the device B_{flat} was set to 1.0.

To evaluate performance, we calculated the average power consumption for the test image set after backlight local dimming as follows:

$$\overline{\mathrm{Power}} = \frac{1}{P \cdot K} \sum_{p=1}^{P} \sum_{k=1}^{K} B_{k,p}, \tag{18}$$

where P is the number of images in the test image set and $B_{k,p}$ is the power of the k-th LED at the p-th image. Also, we calculated the average PSNR for the test image set to compare the distortion to the previous methods and this can be expressed as follows:

$$\begin{aligned} \overline{\mathrm{PSNR}} &= 10 \cdot \log_{10}\left(\frac{1}{\overline{\mathrm{MSE}}}\right) \\ &= 10 \cdot \log_{10}\left(\frac{1}{\frac{1}{P}\sum_{p=1}^{P} \mathrm{MSE}(p)}\right) \end{aligned} \tag{19}$$

where $\mathrm{MSE}(p)$ denotes the mean square error (MSE) value at the p-th image. When we calculated PSNR, we compared the resulting displayed image to the reference image in the simulation tool.

A. Comparison of Fitting Errors for Modeled LSFs

We designed three LSFs to present the backlight spreading patterns from an LED, as mentioned in Section II-A. The three LSFs were fitted to the measured distribution of the backlight luminance from the commercially available smartphone with 50% of power to all LEDs. However, since the measure errors occurred near the center area, as described in the previous section, we attempted to check the effect of the measure error indirectly in the following manner—we selected the best LSF model by fitting the LSF models to the same measured backlight distribution in three ways: i) to the original measured distribution; ii) to the original measured distribution, except the center area; and iii) to the measured distribution whose values near the center are subtracted by a Gaussian distribution fitted to the center area of the measured distribution. We obtained the same results for all three cases of selecting the best LSF in terms of fitting errors, and thus we expect that the measured distribution with error does not greatly change the result of choosing the best or most suitable LSF. Table I shows the result of the fitting error of the three LSFs for the original measured distribution. The fitting error was measured from the MSE. Among the three LSFs, LSF 1 and 3 had the same fitting errors because they have the same distribution of backlight luminance at the same power for all LEDs. However, the LSF 1 is not suitable for the local dimming because it works like global dimming. For the LSF 2, which had the highest fitting error, the luminance on the center area was bright from the superposition of the lights from many LEDs. On the other hand, the luminance on the corner of the display was relatively darker than that of the center area because the number of influencing LEDs is small. Therefore, it was not easy to fit this model to the measured backlight luminance. For the LSF 3, an LED covers the narrow area on the backlight surface, and a pixel is influenced by the smaller number of LEDs. Also, the fitting error was small. Therefore, the effect of local dimming by the LSF 3 could be increased, and we simulated the proposed local dimming algorithm based on the LSF 3 to compare it with other methods.

TABLE I
Fitting Error of LSFs for Measured Backlight Luminance

	LSF 1	LSF 2	LSF 3
MSE ($\cdot 10^{-5}$)	2.373	4.503	2.373

B. Performance Comparison of Backlight Dimming

We compared the proposed method to Lai's method [14], Cho's method [19], Zhang's method [21], and Burini's methods [32], [33]. Although the method of [14] is a global dimming method, we applied this method independently to each of the blocks obtained by dividing the entire display by the number of LEDs in order to operate it as a local dimming method for fair comparison. The value of the fixed weight factor q in [32] and [33] was set from 100 to 800, and the value of allowable distortion α in the proposed method was set from 0.05 to 0.3, experimentally. Also, to reduce the computational time for the proposed method and the methods of [32] and [33], we sampled the pixels in an image every four pixels uniformly in both the horizontal and vertical direction. The LSF 3 was used to compare the performance of the local dimming as written in

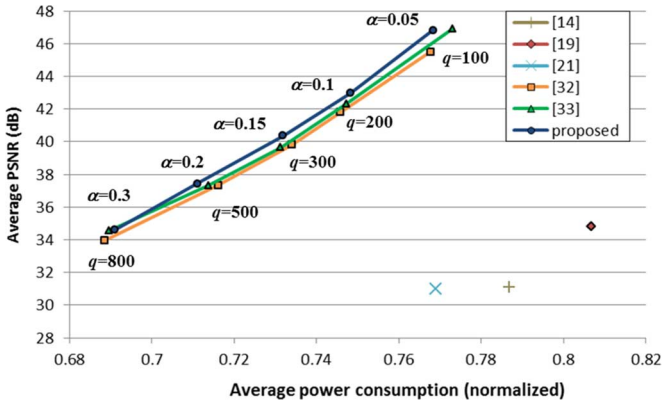

Fig. 5. Comparison of the average PSNR performances for the test image set.

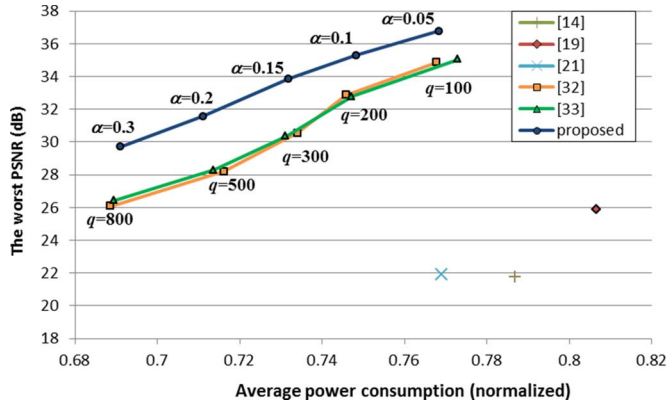

Fig. 6. Comparison of the worst PSNR performances for the test image set.

Section II-A. In other words, if an LED turns on, the light is spread in a straight forward direction without attenuation.

As mentioned in the previous section, since mobile devices at present do not support controlling the power of each LED individually, it is not certain whether the expected LSF from the measured data is exactly matched to the spreading pattern of a single LED in the device we measured. Therefore, instead of experimenting in the actual environment, we performed the backlight local dimming methods and compared the results in the simulation environment.

Fig. 5 shows the result of the average PSNR for the test data set with average power consumption. In the result, the proposed method had a higher average PSNR than the previous methods over 40 dB, which is the level at which people cannot easily perceive distortion when the average power consumption is similar. In other words, if the average PSNR is the same, we can reduce the power consumption more. The methods of [32] and [33] yielded very similar results because of their similar formulation, with the exception of the number of variables. Also, in the results of the methods of [32] and [33], the performances were poor, especially for the images that have a small number of bright pixels with a dark background, because the algorithm determines very low power consumption and many distorted pixels were shown in the resulting displayed image. Other previous methods yielded poorer performance because they heuristically compute the power consumption using a luminance histogram [14] or low-level features such as the average and maximum luminance pixel values [19], [21] without solving optimization problems.

Also, the result for the worst PSNR in the test image set is shown in Fig. 6. The worst PSNR is defined as the lowest PSNR of the resulting displayed image in the test image set. The result shows that the proposed method had better performance than the heuristic methods [14], [19], [21] and also yielded at least a 2 dB-higher PSNR in the worst case compared with [32] and [33]. This shows that the proposed method possesses less risk of large image-dependent performance degradation than with the methods of [32] and [33]. If the weight factor q in [32] and [33] is adjusted to increase the worst PSNR to that of the result of the proposed method, at least 2% more power will be consumed, as shown in Fig. 6. We could see this better when we compared the distribution of PSNR for the test images under

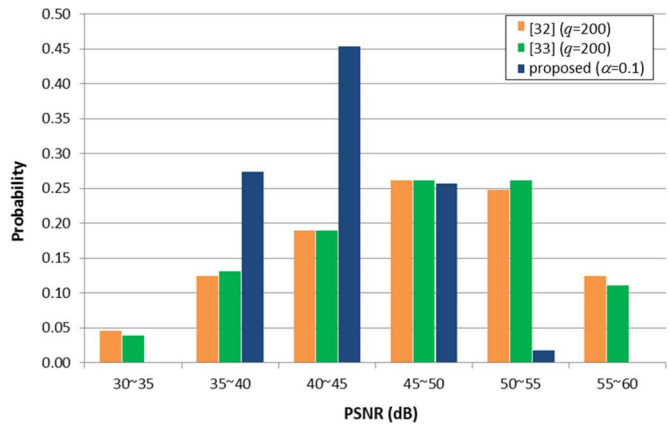

Fig. 7. Comparison of the distribution of PSNR for the test images under the condition of similar average power consumption.

the condition of a similar average power consumption, as shown in Fig. 7. The three heuristic methods [14], [19], [21], were excluded because the average power consumption is not adjustable with these methods. In the methods of [32] and [33], there were low PSNRs for the images whose backgrounds were dark. These images had low power consumption and a high amount of distortion because the amount of distortion could not be controlled adaptively with a fixed weight factor. On the other hand, since the proposed method determined the power of LEDs with distortions under the allowed amount of distortion, the distribution of PSNRs was more concentrated on the average PSNR. Therefore, the image quality fluctuation with the proposed method was smaller than with the methods of [32] and [33].

Fig. 8 shows two resulting displayed images ("*Nightcity*" and "*Kodim23*") from the test image set under the condition of a similar average power consumption. Note that the percentage under each image is the ratio of power consumption after dimming compared with the original power consumption, which is a user-defined brightness of the device B_{flat}. In the "*Nightcity*" image in Fig. 8(a), the pixel values at the streetlights in the red box were more distorted in previous methods than with the proposed method, implying that the proposed method yielded higher PSNR values under similar power consumption. In the "*Kodim23*" image in Fig. 8(b), we could see the distortions, where the color of the bird in the red box was different in the results for [14], [19], and [21]. On the other hand, the results

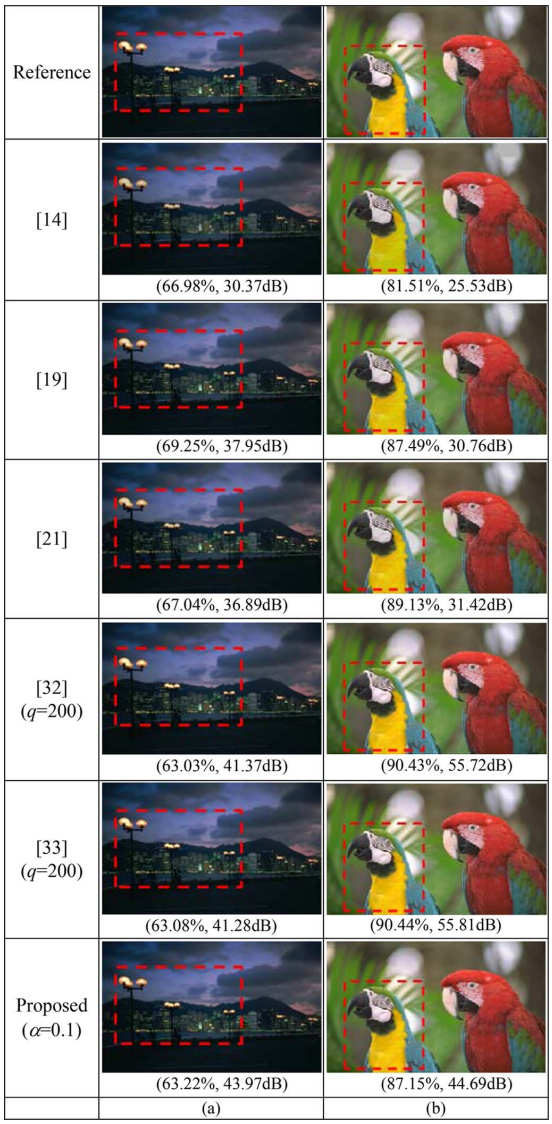

Fig. 8. Resulting displayed image comparison of two images under similar average power consumption. (a) "*Nightcity*." (b) "*Kodim23*."

for [32] and [33] had a very high PSNR (over 55 dB) and the power consumption was higher than with the proposed method. However, we cannot perceive the distortion easily in the result of the proposed method. Therefore, there is no need to have such a high PSNR with high power consumption, and this shows that the methods of [32] and [33] cannot control the amount of distortion better than the proposed method.

Table II shows the comparison of the computation times of the backlight dimming. The average computation time of [32] was too slow even though we sampled the pixels in an image every four pixels in both the horizontal and vertical direction. This is because the method uses so many variables and a high number of iterations when the linear programming works. The method of [33] had a much reduced computation time compared with [32] because a smaller number of variables was used to solve the optimization problem. Nevertheless, the method of [33] was slower than the proposed method by three times because of the slow convergence rate during iteration. The other previous methods were faster than the proposed method, but the performances of the power consumption and PSNR were poor, as shown in Figs. 5 and 6.

TABLE II
AVERAGE COMPUTATION TIME OF BACKLIGHT LOCAL DIMMING

[14]	[19]	[21]	[32] (q=200)	[33] (q=200)	Proposed method (α=0.1)
0.015s	0.018s	0.099s	20.48s	0.403s	0.137s

IV. CONCLUSION

An efficient optimization-based backlight local dimming method for edge-lit LED backlight LCDs is proposed to save power consumption in mobile devices. The LSF is modeled using the measurement of the distribution of backlight luminance, and the optimal power for each LED is determined based on the steepest descent method under the inequality constraint of the given allowable distortions in order to reduce image quality fluctuations. The simulation results show that the proposed method exhibits better performance than previous methods at the unnoticeable level of the difference between the displayed images before and after dimming, and that it reduces the risk of large performance degradations for some images. Also, if the power of each LED can be controlled individually, the proposed method can be used not only in the edge-lit LED backlight, but also in the direct-lit LED backlight because it only requires the position of the LEDs and the modeling information of LSF in LED-backlit LCDs.

REFERENCES

[1] I. Choi, H. Shim, and N. Chang, "Low-power color TFT LCD display for hand-held embedded systems," in *Proc. Int. Symp. Low-Power Electron. Des.* , Aug. 2002, pp. 112–117.
[2] M. H. Crawford, "LEDs for solid-state lighting: Performance challenges and recent advances," *IEEE J. Sel. Topics Quantum Electron.*, vol. 15, no. 4, pp. 1028–1040, Jul./Aug. 2009.
[3] N. Tansu *et al.*, "III-nitride photonics," *IEEE Photon. J.*, vol. 2, no. 2, pp. 241–248, Apr. 2010.
[4] R. M. Farrell, E. C. Young, F. Wu, S. P. DenBaars, and J. S. Speck, "Materials and growth issues for high-performance nonpolar and semipolar light-emitting devices," *Semicond. Sci. Technol.*, vol. 27, no. 2, Feb. 2012, Art. ID 024001.
[5] R. A. Arif, Y.-K. Ee, and N. Tansu, "Polarization engineering via staggered InGaN quantum wells for radiative efficiency enhancement of light emitting diodes," *Appl. Phys. Lett.*, vol. 91, no. 9, 2007, Art. ID 091110.
[6] H. Zhao, G. Liu, J. Zhang, J. D. Poplawsky, V. Dierolf, and N. Tansu, "Approaches for high internal quantum efficiency green InGaN light-emitting diodes with large overlap quantum wells," *Opt. Express*, vol. 19, no. S4, pp. A991–A1007, Jul. 2011.
[7] C.-K. Tan and N. Tansu, "Nanostructured lasers: Electrons and holes get closer," *Nat. Nanotechnol.*, vol. 10, no. 2, pp. 107–109, Feb. 2015.
[8] Y.-K. Ee, J. M. Biser, W. Cao, H. M. Chan, R. P. Vinci, and N. Tansu, "Metalorganic vapor phase epitaxy of III-Nitride light-emitting diodes on nanopatterned AGOG sapphire substrate by abbreviated growth mode," *IEEE J. Sel. Topics Quantum Electron.*, vol. 15, no. 4, pp. 1066–1072, Jul./Aug. 2009.
[9] Y. Ki *et al.*, "Defect-reduced green GaInN/GaN light-emitting diode on nanopatterned sapphire," *Appl. Phys. Lett.*, vol. 98, no. 15, 2011, Art. ID 151102.
[10] S. Choi *et al.*, "Efficiency droop due to electron spill-over and limited hole injection in III-nitride visible light-emitting diodes employing lattice-matched InAlN electron blocking layers," *Appl. Phys. Lett.*, vol. 101, no. 16, 2012, Art. ID 161110.
[11] G. Liu, J. Zhang, C.-K. Tan, and N. Tansu, "Efficiency-droop suppression by using large-bandgap AlGaInN thin barrier layers in InGaN quantum-well light-emitting diodes," *IEEE Photon. J.*, vol. 5, no. 2, Apr. 2013, Art. ID 2201011.

[12] H. Zhao, G. Liu, J. Zhang, R. A. Arif, and N. Tansu, "Analysis of internal quantum efficiency and current injection efficiency in III-Nitride light-emitting diodes," *J. Display Technol.*, vol. 9, no. 4, pp. 212–225, Apr. 2013.
[13] H. G. Hulze and P. DeGreef, "Power savings by local dimming on a LCD panel with side lit backlight," in *SID Symp Dig Tech Papers*, Jun. 2009, vol. 40, no. 1, Art. ID 749752.
[14] C.-C. Lai and C.-C. Tsai, "Backlight power reduction and image contrast enhancement using adaptive dimming for global backlight applications," *IEEE Trans. Consumer Electron.*, vol. 54, no. 2, pp. 669–674, May 2008.
[15] S. J. Kang and Y. H. Kim, "Image integrity-based gray-level error control for low power liquid crystal displays," *IEEE Trans. Consum. Electron.*, vol. 55, no. 4, pp. 2401–2406, Nov. 2009.
[16] S. J. Kang and Y. H. Kim, "Multi-histogram-based backlight dimming for low power liquid crystal displays," *J. Display Technol.*, vol. 7, no. 10, pp. 544–549, Oct. 2011.
[17] S. I. Cho, S.-J. Kang, and Y. H. Kim, "Image quality-aware backlight dimming with color and detail enhancement techniques," *J. Display Technol.*, vol. 9, no. 2, pp. 112–121, Feb. 2013.
[18] Q. Feng, H. Tong, and G. Lv, "An adaptive global LED backlight dimming for contrast enhancement and power reduction," *Solid State Phenomena*, vol. 181–182, pp. 241–244, 2012.
[19] H. Cho and O. Kwon, "A backlight dimming algorithm for low power and high image quality LCD applications," *IEEE Trans. Consumer Electron.*, vol. 55, no. 2, pp. 839–844, May 2009.
[20] W. S. Oh, D. Cho, K. M. Cho, G. W. Moon, B. Yang, and T. Jang, "A novel two-dimensional adaptive dimming technique of X-Y channel drivers for LED backlight system in LCD TVs," *J. Display Technol.*, vol. 5, no. 1, pp. 20–26, Jan. 2009.
[21] X. B. Zhang, R. Wang, D. Dong, J. H. Han, and H. X. Wu, "Dynamic backlight adaptation based on the details of image for liquid crystal displays," *J. Display Technol.*, vol. 8, no. 2, pp. 108–111, Feb. 2012.
[22] H. Nam, "Low power active dimming liquid crystal display with high resolution backlight," *Electron. Lett.*, vol. 47, no. 9, pp. 538–540, Apr. 2011.
[23] M. Albrecht, A. Karrenbauer, T. Jung, and C. Xu, "Sorted sector covering combined with image condensation—An efficient method for local dimming of direct-lit and edge-lit LCDs," *IEICE Trans. Electron.*, vol. 93, no. 11, pp. 1556–1563, 2010.
[24] H. Jung, Y. Lee, B. Choi, and D. Y. Suh, "Cooperative local dimming for accurate backlight brightness matching," *Electron. Lett.*, vol. 47, no. 4, pp. 252–254, Feb. 2011.
[25] D. Cho, W.-S. Oh, and G. W. Moon, "A novel adaptive dimming LED backlight system with current compensated X-Y channel drivers for LCD TVs," *J. Display Technol.*, vol. 7, no. 1, pp. 29–35, Jan. 2011.
[26] H. Cho and O. K. Kwon, "A local dimming algorithm for low power LCD TVs using edge-type LED backlight," *IEEE Trans. Consumer Electron.*, vol. 56, no. 4, pp. 2054–2060, Nov. 2010.
[27] Q. Cui, P. He, X. Guo, J. Lu, G. Liang, and Y. Su, "HSP: A hybrid simulation platform for backlight dimming in TFT-LCDs," in *SID Symp. Dig. Tech. Papers*, May 2010, vol. 41, no. 1, pp. 1544–1547.
[28] J. J. Hong, S. E. Kim, and W. J. Song, "A clipping reduction algorithm using backlight luminance compensation for local dimming liquid crystal displays," *IEEE Trans. Consum. Electron.*, vol. 56, no. 1, pp. 240–246, Feb. 2010.
[29] H. Chen, J. Sung, T. Ha, Y. Park, and C. Hong, "Backlight local dimming algorithm for high contrast LCD-TV," in *Proc. ASID*, Oct. 2006, pp. 168–171.
[30] H. Chen, J. Sung, T. Ha, and Y. Park, "Locally pixel-compensated backlight dimming for improving static contrast on LED backlight LCDs," in *SID Symp. Dig. Tech. Papers*, May 2007, vol. 38, no. 1, pp. 1339–1342.
[31] C. H. Lee, W. H. Shaw, H. I. Liao, S. L. Yeh, and H. H. Chen, "Local dimming of liquid crystal display using visual attention prediction model," in *Proc. Int. Conf. Comput. Commun. Networks*, Jul. 2011, pp. 1–6.
[32] N. Burini, E. Nadernejad, K. Korhonen, S. Forchhammer, and X. Wu, "Image dependent energy-constrained local backlight dimming," in *Proc. IEEE Int. Conf. Image Process.*, Sep. 2012, pp. 2797–2800.
[33] N. Burini, E. Nadernejad, J. Korhonen, S. Forchhammer, and X. Wu, "Modeling power-constrained optimal backlight dimming for color displays," *J. Display Technol.*, vol. 9, no. 8, pp. 656–665, Aug. 2013.
[34] S. Jung, M. Kim, D. Kim, and J. Lee, "Local dimming design and optimization for edge-type LED backlight unit," in *SID Symp. Dig. Tech. Papers*, Jun. 2011, vol. 42, no. 1, pp. 1430–1432.
[35] Y. K. Han and W. J. Song, "A backlight simulator for an edge-type backlight unit in local dimming systems," in *Proc. IEEE Int. Conf. Consumer Electron.*, Jan. 2011, pp. 655–656.
[36] D. G. Luenberger, *Linear and Nonlinear Programming*. Reading, MA, USA: Addison-Wesley, 1984.
[37] G. H. Hostetter, M. S. Santina, and P. D'Carpio-Montalvo, *Analytical, Numerical and Computational Methods for Science and Engineering*. Englewood Cliffs, NJ, USA: Prentice-Hall, 1991.
[38] Kodak Lossless True Color Image Suite. Nov. 1999 [Online]. Available: http://r0k.us/graphics/kodak/
[39] ISO12640-2 . [Online]. Available: http://www.iso.org/
[40] Canon dataset. [Online]. Available: http://www.cipr.rpi.edu/resource/stills/canon.html
[41] "MPEG-2 HD test patterns," [Online]. Available: www.w6rz.net/

Seungwook Cha received the B.S. degree in electronic engineering from the Korea University, Seoul, Korea, in 2006. He is currently working towards the M.S. and Ph.D. joint degree in electrical engineering at Korea University. His research interests are image and video signal processing, digital broadcasting, and other issues on image and video technologies.

Taehyeon Choi received the B.S. degree in electronic engineering from Hoseo University, Asan, Korea, in 2008, and the M.S. degree in image engineering from the Chung-Ang University, Seoul, Korea, in 2011. He is currently working toward the Ph.D. degree in electrical engineering at Korea University. His research interests are image and video signal processing, digital broadcasting, and other issues on image and video technologies.

Hoonjae Lee received the B.S. degree in electronic engineering from the Korea University, Seoul, Korea, in 2006. He is currently working towards the M.S. and Ph.D. joint degree in electrical engineering at Korea University. His research interests are image and video signal processing, digital broadcasting, and other issues on image and video technologies.

Sanghoon Sull (S'79–M'81–SM'13) received the B.S. degree with honors in electronics engineering from the Seoul National University, Korea, in 1981, the M.S. degree in electrical engineering from the Korea Advanced Institute of Science and Technology in 1983, and Ph.D. degree in electrical and computer engineering from the University of Illinois at Urbana-Champaign, in 1993. In 1983–1986, he was with the Korea Broadcasting Systems, working on the development of the teletext system. In 1994–1996, he conducted research on motion analysis at the NASA Ames Research Center. In 1996–1997, he conducted research on video indexing/browsing and was involved in the development of the IBM DB2 Video Extender at the IBM Almaden Research Center. He joined the School of Electrical Engineering at the Korea University as an Assistant Professor in 1997 and is currently a Professor. His current research interests include image/video processing, computer vision, data analysis, and their applications to 3D TV and smart phone.